



Discovery of 3,9-diazabicyclo[4.2.1]nonanes as potent dual orexin receptor antagonists with sleep-promoting activity in the rat

Paul J. Coleman^{a,*}, John D. Schreier^a, Anthony J. Roecker^a, Swati P. Mercer^a, Georgia B. McGaughey^b, Christopher D. Cox^a, George D. Hartman^a, C. Meacham Harrell^c, Duane R. Reiss^c, Scott M. Doran^c, Susan L. Garson^c, Wayne B. Anderson^d, Cuyue Tang^d, Thomayant Prueksaritanont^d, Christopher J. Winrow^c, John J. Renger^c

^a Department of Medicinal Chemistry, Merck Research Laboratories, PO Box 4, Sumneytown Pike, West Point, PA 19486, United States

^b Chemistry Modeling and Informatics, Merck Research Laboratories, PO Box 4, Sumneytown Pike, West Point, PA 19486, United States

^c Department of Depression and Circadian Disorders, Merck Research Laboratories, PO Box 4, Sumneytown Pike, West Point, PA 19486, United States

^d Department of Drug Metabolism, Merck Research Laboratories, PO Box 4, Sumneytown Pike, West Point, PA 19486, United States

ARTICLE INFO

Article history:

Received 16 April 2010

Revised 10 May 2010

Accepted 12 May 2010

Available online 25 May 2010

Keywords:

Sleep

Insomnia

Diazepane

GPCR antagonist

Brain penetration

Orexin

Receptor

ABSTRACT

Orexins are excitatory neuropeptides that regulate arousal and sleep. Orexin receptor antagonists promote sleep and offer potential as a new therapy for the treatment of insomnia. In this Letter, we describe the synthesis of constrained diazepanes having a 3,9 diazabicyclo[4.2.1]nonane bicyclic core with good oral bioavailability and sleep-promoting activity in a rat EEG model.

© 2010 Elsevier Ltd. All rights reserved.

Orexins are excitatory neuropeptides that bind to two G-protein coupled receptors (GPCRs), orexin-1 (OX1R) and orexin 2 (OX2R).¹ Neurons that secrete orexins project from the lateral hypothalamus and innervate diverse regions of the central nervous system that govern sleep, behavioral arousal, and stability of the wake state. Based on genetic studies and a clear link to the pathophysiology of narcolepsy, orexin antagonists have been explored as a potential novel treatment for sleep disorders.² Indeed, a dual orexin antagonist has recently been reported to be sleep-promoting in rodents, dogs, and in human subjects.³

In previous publications from this laboratory, we described the discovery of a novel series of diazepane dual orexin receptor antagonists including 2-[4-[5-methyl-2-(2*H*-1,2,3-triazolyl-2-yl)benzoyl]-1,4-diazepan-1-yl]quinazoline, **1**.⁴ Compound **1** (Fig. 1) has high affinity for both orexin receptors but has low bioavailability (<10%) following oral administration to rats. Spectroscopic, X-ray, and molecular modelling studies indicate that *N,N*-1,4-diazepane antagonists such as **1** adopt a low energy conformation that is characterized by an intramolecular π -stacking interaction and a twist-

boat conformation.⁵ Based on this knowledge we designed constrained diazepanes such as **2** that enforce the aryl–aryl interaction present in compound **1**. These bridged diazepanes are constrained by inclusion of a one-carbon bridge.⁶ Despite maintaining excellent potency against OX1R and OX2R, these constrained analogs also had poor preclinical pharmacokinetics with high plasma clearance and low bioavailability. In this Letter, we describe the synthesis of constrained diazepanes with two-carbon bridges. These efforts were rewarded by the discovery of an orexin antagonist with a 3,9-diazabicyclo[4.2.1]nonane core **8a** that has improved oral bioavailability and sleep-promoting activity in a rat EEG model.

We sequentially varied the linkage of a two-carbon bridge on the seven-membered diazepane ring. We synthesized these analogs by reaction sequences detailed in Schemes 1 and 2. In preparing these orexin antagonists, we maintained the 6-fluoroquinazoline and 5-methyl-2-triazolylbenzamide as preferred, potency-enhancing features. The 3,9-diazabicyclo[4.2.1]nonane core was synthesized as shown in Scheme 1. Schmidt reaction with the *N*-benzyl-3-nor-tropinone **3** afforded the bicyclic lactam **4** in excellent yield. Lactam reduction followed by manipulation of amine protecting groups provided bicyclic diamine **5**. Amide formation, BOC-removal, and nucleophilic aromatic substitution reaction provided receptor

* Corresponding author. Tel.: +1 215 652 4618.

E-mail address: paul_coleman@merck.com (P.J. Coleman).

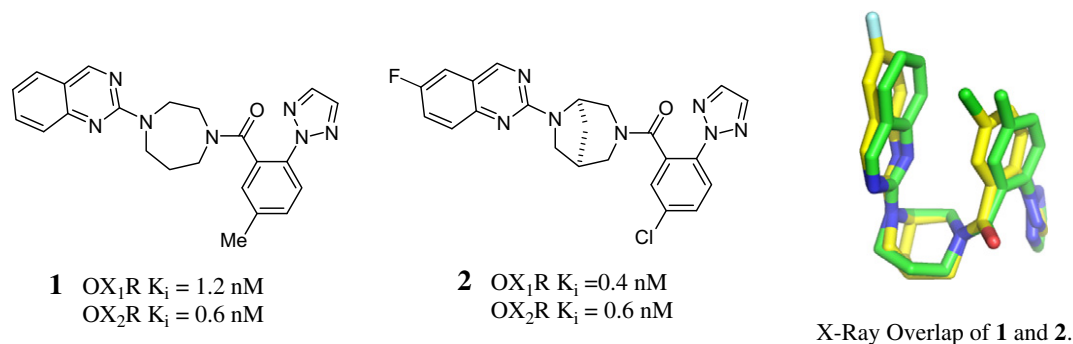


Figure 1. Structure and X-ray superimposition of orexin receptor antagonists **1** and **2**.

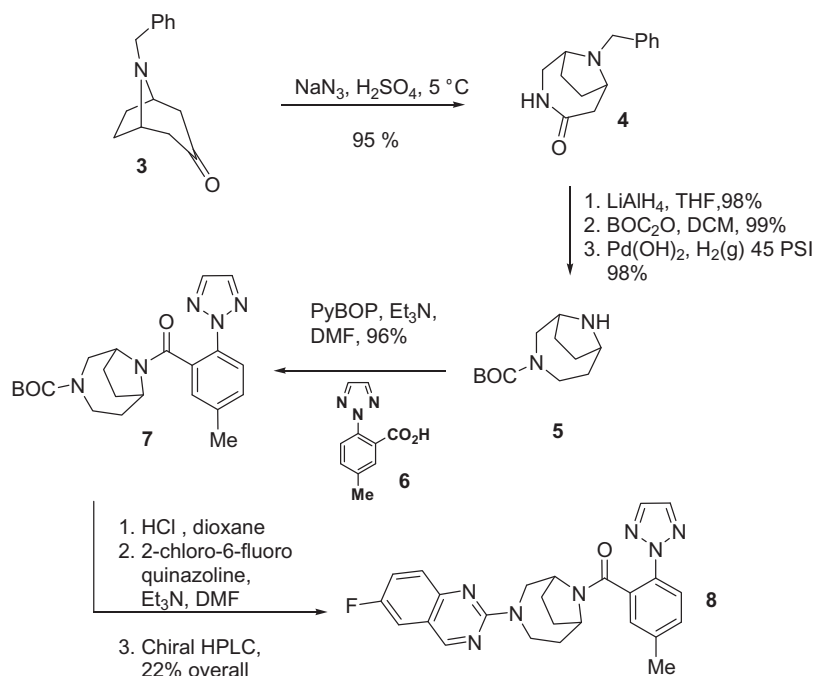
antagonist **8**. Reordering the heteroarylation and amide formation steps afforded the isomeric diazabicyclo[4.2.1]nonane derivative **9**. Compound *rac*-**8** could be resolved by HPLC on a chiral stationary support to afford enantiomers **8a** and **8b**.⁷

For compounds shown in Scheme 2, we began the synthesis with a catalytic, asymmetric aza-Diels–Alder reaction to produce **11** in high yield and enantioselectivity.⁸ Bicyclic piperidone **11** was then treated sodium azide under Schmidt conditions to provide a separable mixture of the two bicyclic lactams **12** and **13**. Lactam **12** was reduced with lithium aluminum hydride and the protected diazepane treated with 2-chloro-6-fluoroquinazoline. Removal of the PMP group with ceric ammonium nitrate (CAN) followed by amide coupling with **6** afforded **14a**. Reordering the heteroarylation and amide coupling reactions provides the bridged compound **15a**. The sequence shown in Scheme 2 was then repeated using D-proline as an amino acid catalyst and provided stereoisomers **14b** and **15b**. The (1*R*,5*R*)-2,6 diazabicyclo[3.2.2]nonane **16a** was derived from a D-proline catalyzed Diels–Alder reaction affording *ent*-**11** (scheme not shown). Subsequent transformations afforded **16a**.⁹ This sequence was repeated with L-proline as the asymmetric catalyst and provided (1*S*,5*S*)-2,6-diazabicyclo[3.2.2]nonane **16b**.

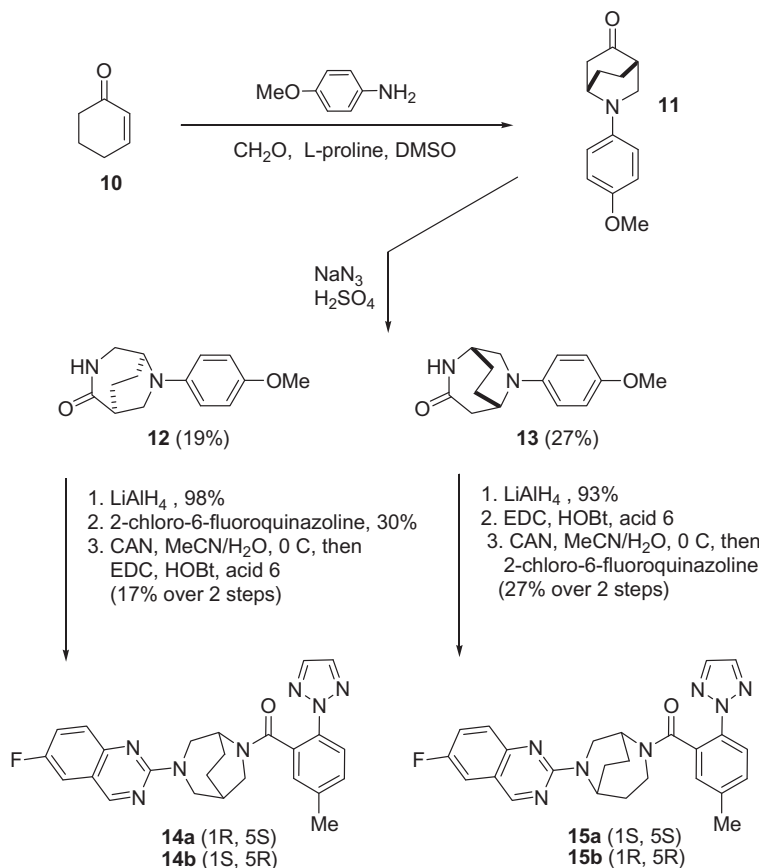
Constraining the diazepanes by installation of various two-carbon bridges provided several potent compounds including com-

pounds **8a**, **9**, and **16a** (Table 1). Nearly all of these bridged analogs maintained balanced potency on OX1R and OX2R. Interestingly, constrained diazepane **14b** represents an exception and gained selectivity for OX1R over OX2R. Although selected diazepanes with two-carbon bridges tended to retain potency in the OX1R and OX2R binding assays, FLIPR potencies were more highly shifted than unconstrained diazepanes (FLIPR IC₅₀/binding K_i = 160–340× for **8a** vs 24–45× shift for **1**). We attributed this shift to greater lipophilicity and higher nonspecific binding in the FLIPR assay. The measured Log P for **8a** is higher than for **1** (>3.4 vs 2.9, respectively) while polar surface area was comparable (71 Å² for **8a** and 74 Å² for **1**). Passive cellular permeability remained high for these analogs (*P*_{app} >25 × 10^{−6} cm/s; LLC-PK1 cells).

We were unable to generate diffraction quality crystals from any of the 2-carbon bridged compounds and ¹H NMR spectra for these molecules were highly complex with multiple conformers in equilibrium.¹⁰ However, modeling studies with **8a** provided a minimized structure that has a favorable aryl–aryl interaction and superimposes on the X-ray of compound **1**.¹¹ These results agree with earlier studies that suggest enforcing the π-stacking array in the diazepane series leads to a highly favorable binding interaction with the orexin receptors.^{5,6}



Scheme 1. Synthesis of 3,9-diazabicyclo[4.2.1]nonanes as orexin receptor antagonists.



Scheme 2. Synthesis of 3,6-diazabicyclo[3.2.2]nonanes and 2,6-diazabicyclo[3.2.2]nonanes as orexin receptor antagonists.

The most promising compounds identified from these studies were further characterized in terms of the pharmacokinetic properties, brain penetration, and in vivo evaluation. In vitro microsomal studies of related diazepane analogs suggested that human and dog hepatic stability would be similar (and dissimilar from rat). Therefore we emphasized low plasma clearance in the dog as a criterion for selecting compounds for additional studies.

The plasma clearance of **8a** was low in the dog following intravenous administration ($Cl = 3.6$ mL/min/kg) and more favorable than reference compound **1** ($Cl = 12$ mL/min/kg) or other bridged compounds **9** ($Cl = 11$ mL/min/kg) and **16** ($Cl = 14$ mL/min/kg). Indeed when dosed orally to dogs, compound **8a** had excellent bioavailability ($F = 100\%$), with a C_{max} of 3.4 μ M (Table 2).

Steady state plasma, brain, and cerebrospinal fluid (CSF) concentrations of compound **8a** were assessed in anesthetized Sprague-Dawley rats.¹² Compound **8a** was administered to rats by intravenous infusion in HPCD at 2 mg/kg, the animals were sacrificed at 30 min; brain, plasma, and CSF levels were measured. Plasma and brain levels reached 1455 nM and 584 nM, respectively (brain/plasma = 0.40). At this dose, CSF levels of **8a** were below the limits of quantitation, consistent with the very high levels of plasma protein binding measured in the rat (99.6% bound). Compound **8a** was not a substrate of the P-glycoprotein transporter.¹³

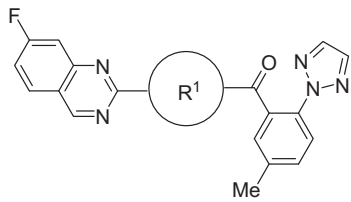
CSF concentrations of **8a** were quantified as a surrogate measure of receptor-available free compound in the brain.¹⁴ In order to select an appropriate dose for in vivo pharmacodynamic evaluation in the rat, we explored a range of oral doses in the rat and directly measured rat plasma and CSF levels at single time points (1 – 2 h; Table 3). After oral administration of **8a**, plasma exposures in the rat increased nonlinearly from 10 to 60 mg/kg while the CSF/plasma ratio ranged from 0.004 to 0.011 consistent with an un-

bound plasma concentration of 0.4% in the rat. Based on these prospective rat PK experiments, a dose of 60 mpk was chosen for in vivo evaluation providing plasma and CSF exposures of 14.6 μ M and 0.17 μ M at 1 h after oral administration. At this dose the CSF concentration of compound **8a** is similar to the FLIPR IC_{50} concentrations in the OX1R and OX2R assays.

Based on favorable rat brain penetration and oral bioavailability in both rats and dogs, **8a** was evaluated in a rat sleep model¹⁵ using telemetric recording of electrocorticogram (ECoG) and electromyogram (EMG) signals to assess time spent in various states of arousal, including active wake, light sleep REM sleep, and delta or slow wave sleep (SWS). Compound **8a** was dosed orally at 60 mg/kg/day to telemetry-implanted rats in their active phase (lights off) and the amount of time spent in each wake/sleep state was measured and binned into 30 min intervals and compared to vehicle treated rats. In this assay, compound **8a** decreased wakefulness in the treated rats for greater than 4 h and sustained increases in slow wave and REM sleep for 3.5 and 6 h, respectively. A lower dose (30 mpk) of **8a** was not efficacious in promoting rat sleep.¹⁶

In conclusion, we have continued to drive the design of our 1,4-diazepane orexin receptor antagonists based on an understanding of the solution and solid state conformations of these systems. Earlier efforts to enforce an energetically favorable π -stacking interaction with one-carbon bridged diazepanes provided analogs with comparable potency to **1** but lacking acceptable pharmacokinetics. The current study demonstrates that the introduction of a two-carbon constraint can significantly improve pharmacokinetics in both rats and dogs while maintaining excellent dual orexin receptor potency. 3,9-Diazabicyclo[4.2.1]nonane **8a** promotes sleep in EEG-telemetered rats at 60 mg/kg when dosed orally; dose selection for this experiment was informed by direct measurements of

Table 1
2-Carbon bridged diazepane orexin antagonists



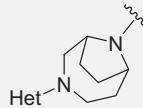
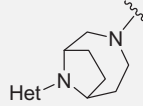
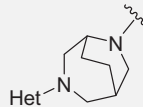
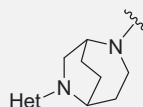
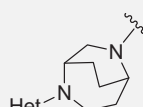
Compound	R ¹	OX1R (K _i , nM)	OX2R (K _i , nM)	FLIPR	
				OX1R (IC ₅₀ , nM)	OX2R (IC ₅₀ , nM)
8a (<i>ent</i> A) 8b (<i>ent</i> B)		0.6 3.7	0.4 6.7	98 99	136 150
9 (<i>rac</i>)		0.9	0.8	72	175
14a (1 <i>R</i> ,5 <i>S</i>) 14b (1 <i>S</i> ,5 <i>R</i>)		10 2.0	2.9 62	104 46	370 790
15a (1 <i>S</i> ,5 <i>S</i>) 15b (1 <i>R</i> ,5 <i>R</i>)		160 345	105 590	2300 1600	1450 >10,000
16a (1 <i>R</i> ,5 <i>R</i>) 16b (1 <i>S</i> ,5 <i>S</i>)		0.6 7.6	2.2 14	125 800	140 740

Table 2
Dog and rat pharmacokinetics for bridged compound **8a** versus **1**

Compd	Species	%F	Cl (mL/min/kg)	T _{1/2} (h)	AUC _{0–24}	C _{max}
1	Dog ^a	16	12	1.3	0.44 μM-h	0.23 μM
	Rat ^b	2	53	0.3	0.19 μM-h	0.30 μM
8a	Dog	100	3.6	1.8	14.11 μM-h	3.4 μM
	Rat	14	23	1.0	1.57 μM-h	0.57 μM

^a Dogs dosed orally at 3 mpk po in PEG200 and at 0.125 mpk iv in DMSO.

^b Rats dosed orally at 10 mpk, po in PEG200 and dosed iv at 2 mpk in DMSO.

Table 3
Rat plasma and CSF concentrations for **8a**

Dose	Plasma concn at 2 h (μM)	CSF concn at 2 h (μM)	CSF/plasma
10 mpk	1.1	0.003	0.004
30 mpk	3.1	0.023	0.007
60 mpk	14.6 ^a	0.170	0.011
100 mpk	12.5 ^b	ND	ND

Rats dosed orally in VitE-TPGS at doses specified.

^a Plasma/CSF levels measured at 1 h.

^b Dosed in PEG 400.

CSF levels of **8a** after oral administration. Despite an improved PK profile for **8a**, the introduction of the two-carbon constraint is associated with an increase in lipophilicity and corresponding decreases in unbound plasma and CSF concentrations. The high plasma exposures (14 μM at 1 h) required for **8a** to achieve efficacy in a rat sleep model suggest that achieving appropriate CSF/plasma concentrations of orexin antagonists may be important determi-

nants of in vivo activity. Further studies to reduce plasma protein binding, enhance unbound brain concentrations, and refine pharmacokinetic-pharmacodynamic relationships for orexin receptor antagonists are ongoing.

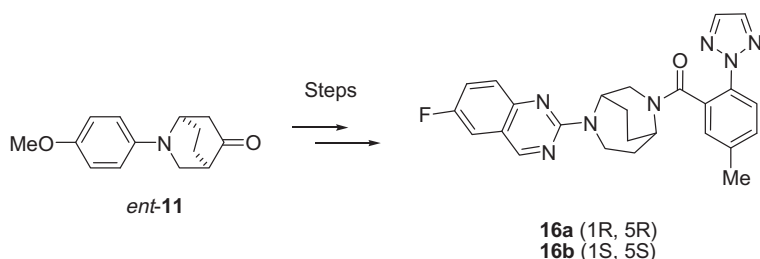
A. Supplementary data

Supplementary data associated with this article can be found, in the online version, at doi:10.1016/j.bmcl.2010.05.047.

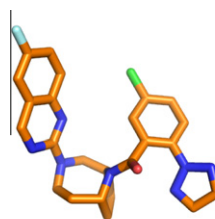
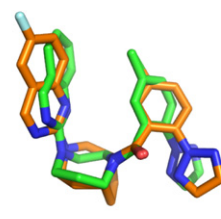
References and notes

- (a) de Lecea, L.; Kilduff, T. S.; Peyron, C.; Gao, X.; Foye, P. E.; Danielson, P. E.; Fukuhara, C.; Battenberg, E. L.; Gautvik, V. T.; Bartlett, F. S.; Frankel, W. N.; van den Pol, A. N.; Bloom, F. E.; Gautvik, K. M.; Sutcliffe, J. G. *Proc. Natl. Acad. Sci.* **1998**, 95, 322; (b) Sakurai, T.; Amemiya, A.; Ishii, M.; Matsuzaki, I.; Chemelli, R. M.; Tanaka, H.; Williams, S. C.; Richardson, J. A.; Kozłowski, G. P.; Wilson, S.; Arch, J. R. S.; Buckingham, R. E.; Haynes, A. C.; Carr, S. A.; Annan, R. S.; McNulty, D. E.; Liu, W.-S.; Terrett, J. A.; Elshourbagy, N. A.; Bergsma, D. J.; Yanagisawa, M. *Cell* **1998**, 92, 573.

2. (a) Boss, C.; Brisbare-Roch, C.; Jenck, F. *J. Med. Chem.* **2009**, *52*, 891; (b) Roecker, A. J.; Coleman, P. J. *Curr. Top. Med. Chem.* **2008**, *8*, 977.
3. Brisbare-Roch, C.; Dingemanse, J.; Koberstein, R.; Hoefer, P.; Aissaoui, H.; Flores, S.; Mueller, C.; Nayler, O.; van Gerven, J.; de Haas, S.; Hess, P.; Qiu, C.; Buchmann, S.; Scherz, M.; Weller, T.; Fischli, W.; Clozel, M.; Jenck, F. *Nat. Med.* **2007**, *13*, 150.
4. Whitman, D. B.; Cox, C. D.; Breslin, M. J.; Brashear, K. M.; Schreier, J. D.; Bogusky, M. J.; Bednar, R. A.; Lemaire, W.; Bruno, J. G.; Hartman, G. D.; Reiss, D. R.; Harrell, C. M.; Kraus, R. L.; Li, Y.; Garson, S. L.; Doran, S. M.; Prueksaritanont, T.; Li, C.; Winrow, C. J.; Koblan, K. S.; Renger, J. J.; Coleman, P. J. *ChemMedChem* **2009**, *4*, 1069.
5. Cox, C. D.; McGaughey, G. B.; Bogusky, M. J.; Whitman, D. B.; Ball, R. G.; Winrow, C. J.; Renger, J. J.; Coleman, P. J. *Bioorg. Med. Chem. Lett.* **2009**, *19*, 2997.
6. Coleman, P. J.; Schreier, J. D.; McGaughey, G. B.; Bogusky, M. J.; Cox, C. D.; Hartman, G. D.; Ball, R. G.; Harrell, C. M.; Reiss, D. R.; Prueksaritanont, T.; Winrow, C. J.; Renger, J. J. *Bioorg. Med. Chem. Lett.* **2010**, *20*, 2311.
7. Racemic mixture **8** was resolved by chromatography using a Chiracel AD column eluting with 40% hexanes/ 60% isopropanol with 0.1% diethylamine. Enantiomer **8a** eluted first and **8b** second.
8. Sundén, H.; Ibrahem, I.; Eriksson, L.; Cordova, A. *Angew. Chem., Int. Ed.* **2005**, *44*, 4877.
9. The 2,6-diazabicyclo[3.2.2]nonane derivatives were synthesized from *ent*-**11** by (1) Schmidt reaction (30%); (2) LiAlH₄ reduction, heteroarylation with 2-chloro-6-fluoroquinazoline (60% for two steps); (3) CAN deprotection followed by amide coupling with acid **6** (41% over two steps). The (1*R*,5*S*) isomer was derived from *L*-proline catalyzed Diels–Alder and the (1*S*,5*S*) antipode was derived from same reaction using *D*-proline.



10. The absolute stereochemistry of **8a** has not established by X-ray crystallography. The depiction of **8a** as *R,R* is based on analogy to the X-ray of compound **2** (see Ref.⁵).
11. Conformational searching using the mixed torsion/low-mode sampling algorithm as implemented in Schrödinger, v9.0 (Schrödinger, LLC, v9.0) was performed using the OPLS force field in a constant dielectric of 1. All conformers within 5 kcal/mol of the global minimum were saved and visually inspected for evidence of π -stacking. See: Kolossváry, I.; Guida, W. C. *J. Am. Chem. Soc.* **1996**, *118*, 5011. Minimization of orexin receptor antagonists **8a** and superimposition with X-ray of **1** are shown below.

Minimized **8a**Superimposition of **8a** and **1**

12. Seven to 10 weeks old Sprague-Dawley rats were anesthetized with isoflurane (5% with oxygen at 2 l/min). Once anesthetized, the rat was shaved from the ears to the shoulders and then placed on a circulating water warming blanket set at 37 °C. Anesthesia was maintained using 2% isoflurane by means of a nose cone. The tail vein was cannulated with a 25G winged infusion needle connected via tubing to a syringe containing the test compound. The syringe

was placed on a Harvard Apparatus infusion pump set to deliver 2 mg/kg over 30 min. At the end of the infusion, CSF was collected from the cisterna magna by needle puncture with slow aspiration using a 25G butterfly connected by tubing to a 1 cc syringe. The CSF sample was dispensed into a vial and immediately frozen on dry ice. A 1 ml blood sample was then obtained via cardiac puncture, centrifuged, plasma collected and frozen on dry ice. The brain was rapidly harvested and frozen on dry ice. CSF, plasma, and brain samples were then analyzed to determine compound levels.

13. The MDR1 B-A/A-B ratio for **8b** = 0.7 with an apparent permeability of 29×10^{-6} cm/s in LLC-PK1 cells. For a description of this method see: (a) Hochman, J. H.; Yamazaki, M.; Ohe, T.; Lin, J. H. *Curr. Drug Metab.* **2002**, *3*, 257; (b) Lin, J. H.; Yamazaki, M. *Drug Metab. Rev.* **2003**, *35*, 417.
14. Liu, X.; Smith, B. J.; Chen, C.; Callegari, E.; Becker, S. L.; Chen, X.; Cianfroga, J.; Doran, A. C.; Doran, S. D.; Gibbs, J. P.; Hosea, N.; Liu, J.; Nelson, F. R.; Szewc, M. A.; Deussen, J. V. *Drug Metab. Dispos.* **2006**, *34*, 1443.
15. See Supplementary data for a description of the rat EEG assay.
16. Compound **8a** had no effect on rat sleep when dosed at 30 mpk ip in PEG 200.